USER GUIDE
Planetary-Code-Collection: Thermal and Ice Evolution Models for Planetary Surfaces

Norbert Schörghofer (norbert@hawaii.edu)

2002–2016
Last updated October 9, 2016

Contents

Preface

Companion to https://github.com/nschorgh/Planetary-Code-Collection/

Part 1

Conduction of Heat

1-Dimensional Numerical Model of Thermal Conduction in the Planetary Subsurface

Authors & History: originally implemented by Samar Khatiwala in 2001 (including upper radiation boundary condition for semi-implicit scheme); extended to variable thermal properties and irregular grid by Norbert Schörghofer 2002–2003

1.1 Governing Equation

T ... temperture, t ... time, z ... depth, ρc ... volumetric heat capacity, k ... thermal conductivity

$$\rho c \frac{\partial T}{\partial t} = \frac{\partial}{\partial z}\left(k \frac{\partial T}{\partial z}\right) \tag{1.1}$$

$F = k\dfrac{\partial T}{\partial z}$ ... heat flux
various boundary conditions

1.2 Semi-Implicit Scheme on Irregular Grid

$$\frac{\partial}{\partial z}F_j = \frac{F_{j+\frac{1}{2}} - F_{j-\frac{1}{2}}}{(z_{j+1}-z_{j-1})/2} = 2\frac{k_{j+\frac{1}{2}}\frac{T_{j+1}-T_j}{z_{j+1}-z_j} - k_{j-\frac{1}{2}}\frac{T_j-T_{j-1}}{z_j-z_{j-1}}}{z_{j+1}-z_{j-1}}$$

$$\begin{aligned}(\rho c)_j \frac{\partial T_j}{\partial t} &= \frac{2k_{j+\frac{1}{2}}}{(z_{j+1}-z_j)(z_{j+1}-z_{j-1})}T_{j+1} - \frac{2}{z_{j+1}-z_{j-1}}\left(\frac{k_{j+\frac{1}{2}}}{z_{j+1}-z_j} + \frac{k_{j-\frac{1}{2}}}{z_j-z_{j-1}}\right)T_j + \\ &+ \frac{2k_{j-\frac{1}{2}}}{(z_j-z_{j-1})(z_{j+1}-z_{j-1})}T_{j-1}\end{aligned}$$

$$\text{introduce} \quad \alpha_j = \frac{\Delta t}{(\rho c)_j}\frac{k_{j+\frac{1}{2}}}{(z_{j+1}-z_j)(z_{j+1}-z_{j-1})} \quad \text{and} \quad \gamma_j = \frac{\Delta t}{(\rho c)_j}\frac{k_{j-\frac{1}{2}}}{(z_j-z_{j-1})(z_{j+1}-z_{j-1})} \tag{1.2}$$

$$\Delta t \frac{\partial T_j}{\partial t} = 2\alpha_j T_{j+1} - 2(\alpha_j+\gamma_j)T_j + 2\gamma_j T_{j-1}$$

$$T_j^{n+1} - T_j^n = \alpha_j T_{j+1}^{n+1} - (\alpha_j+\gamma_j)T_j^{n+1} + \gamma_j T_{j-1}^{n+1} + \alpha_j T_{j+1}^n - (\alpha_j+\gamma_j)T_j^n + \gamma_j T_{j-1}^n$$

$$\boxed{-\alpha_j T_{j+1}^{n+1} + (1+\alpha_j+\gamma_j)T_j^{n+1} - \gamma_j T_{j-1}^{n+1} = \alpha_j T_{j+1}^n + (1-\alpha_j-\gamma_j)T_j^n + \gamma_j T_{j-1}^n} \quad 1<j<N \tag{1.3}$$

Superscript n refers to time step. Subscript j refers to position z_j. The conductivity k is defined on half-points. In the program, $2(\rho c)_j = (\rho c)_{j+\frac{1}{2}} + (\rho c)_{j-\frac{1}{2}}$. In this way, the parameters k and ρc do not need to be defined at an interface of two layers with different thermal properties. Since indices in the program must be integers, we choose $k(j) = k_{j-\frac{1}{2}}$ and the same for ρc.

1.2.1 Upper boundary condition:

a) Radiation

$$Q + k \left.\frac{\partial T}{\partial z}\right|_{z=0} = \epsilon\sigma T^4\big|_{z=0} \tag{1.4}$$

Q is the incoming solar flux including the atmospheric contribution.
introduce auxiliary quantity T_0, such that surface temperature $T_s = (T_0 + T_1)/2$

$$\left.\frac{\partial T}{\partial z}\right|_{z=0} = \frac{T_1 - T_0}{\Delta z} \quad \text{and} \quad T^4\big|_{z=0} = \left(\frac{T_0 + T_1}{2}\right)^4 \quad \text{with} \quad \Delta z = 2z_1$$

$T = T_r + T'$ T_r is a reference temperature around which we linearize

$$\begin{aligned} Q + k_{1/2}\frac{T_1 - T_0}{\Delta z} &= \epsilon\sigma\left(\frac{2T_r + T_0' + T_1'}{2}\right)^4 \\ &\approx \epsilon\sigma T_r^4 + 2\epsilon\sigma T_r^3(T_0' + T_1') \\ &= -3\epsilon\sigma T_r^4 + 2\epsilon\sigma T_r^3(T_0 + T_1) \end{aligned}$$

$T_0\left(\frac{k_{1/2}}{\Delta z} + B(T_r)\right) = Q + 3\epsilon\sigma T_r^4 + T_1\left(\frac{k_{1/2}}{\Delta z} - B(T_r)\right)$ where $B(T_r) = 2\epsilon\sigma T_r^3$
introduce $a = (Q + 3\epsilon\sigma T_r^4)/(\frac{k}{\Delta z} + B)$ and $b = (\frac{k_{1/2}}{\Delta z} - B)/(\frac{k_{1/2}}{\Delta z} + B)$

$$-\alpha_1 T_2^{n+1} + (1 + \alpha_1 + \gamma_1 - \gamma_1 b^n)T_1^{n+1} = \alpha_1 T_2^n + (1 - \alpha_1 - \gamma_1 + \gamma_1 b^n)T_1^n + \gamma_1 \frac{Q^n + Q^{n+1} + 6\epsilon\sigma T_r^4}{\frac{k_{1/2}}{\Delta z} + B^n}$$

choose $\Delta z = z_2 - z_1 = 2z_1$, define $\beta = \frac{\Delta t}{(\rho c)_1}\frac{1}{2\Delta z^2}$, then $\alpha_1 = \beta k_{3/2}$ and $\gamma_1 = \beta k_{1/2}$

$$\text{surface temperature} \quad T_s = \frac{1}{2}(T_1 + T_0) = \frac{1}{2}\left(\frac{Q + 3\epsilon\sigma T_r^4}{k_{1/2}/\Delta z + B} + T_1 + bT_1\right) = \frac{Q + 3\epsilon\sigma T_r^4 + \frac{2k}{\Delta z}T_1}{2(k_{1/2}/\Delta z + B)}$$

choose $T_r^n = T_s^{n-1}$
implemented in `conductionQ.f`

b) prescribed T

standard formulas (1.2,1.3) with $T_0 = T_s$ and $z_0 = 0$

$$\alpha_1 = \frac{\Delta t}{(\rho c)_1}\frac{k_{3/2}}{(z_2 - z_1)z_2}, \qquad \gamma_1 = \frac{\Delta t}{(\rho c)_1}\frac{k_{1/2}}{z_1 z_2}$$

$$-\alpha_1 T_2^{n+1} + (1 + \alpha_1 + \gamma_1)T_1^{n+1} = \alpha_1 T_2^n + (1 - \alpha_1 - \gamma_1)T_1^n + \gamma_1(T_s^n + T_s^{n+1})$$

implemented in `conductionT.f`

1.2.2 Lower boundary condition:

(assume $z_{N+1} - z_N = z_N - z_{N-1}$)
No heat flux: $F_{N+\frac{1}{2}} = 0 \quad \Rightarrow \quad k_{N+\frac{1}{2}}(T_{N+1} - T_N) = 0 \quad \Rightarrow \quad T_{N+1} = T_N$

$$(1+\gamma_N)T_N^{n+1} - \gamma_N T_{N-1}^{n+1} = (1-\gamma_N)T_N^n + \gamma_N T_{N-1}^n$$

$$\gamma_N = \frac{\Delta t}{(\rho c)_N} \frac{k_{N-\frac{1}{2}}}{2(z_N - z_{N-1})^2}$$

Or geothermal heating: $F_{N+\frac{1}{2}} = F_{\text{geothermal}} \quad \Rightarrow \quad k_{N+\frac{1}{2}}(T_{N+1} - T_N) = \Delta z F_{\text{geothermal}}$

$$(1+\gamma_N)T_N^{n+1} - \gamma_N T_{N-1}^{n+1} = (1-\gamma_N)T_N^n + \gamma_N T_{N-1}^n + \frac{\Delta t}{(\rho c)_N} \frac{F_{\text{geothermal}}}{\Delta z}$$

1.3 With Frost Cover (Mars)

Add latent heat of CO_2 sublimation

$$Q + k \left.\frac{\partial T}{\partial z}\right|_{z=0} = \epsilon\sigma T^4\big|_{z=0} + L\frac{dm_{CO_2}}{dt} \tag{1.5}$$

call `conductionQ` if T_s is above CO_2 frost point or if $m_{CO_2} = 0$; call `conductionT` if T_s is below CO_2 frost point or if $m_{CO_2} > 0$; calculate energy difference and add CO_2 mass; adjust surface albedo; repeat this at every time step

1.4 Influence of Ice on Thermal Conductivity

This is only one possible parametrization. In retrospective, it agrees well with the laboratory measurements by Siegler et al. (2012).

$$\begin{aligned} \rho c &= (1-\epsilon)\rho_{\text{regolith}} c_{\text{regolith}} + \epsilon f \rho_{\text{ice}} c_{\text{ice}} \\ k &= (1-\epsilon)k_{\text{regolith}} + \epsilon f k_{\text{ice}} + (1-f)\epsilon k_{\text{air}} \end{aligned}$$

ρ ... density; c ... heat capacity; k ... thermal conductivity
ϵ ... porosity (void space / total volume)
f ... ice filling fraction ($f = \rho_f/\rho_{\text{ice}}$, ρ_f =density of free ice)
Observed from orbit is ice-three thermal inertia I.

at around 200 Kelvin: $c_{\text{ice}} \approx 1540$ J/(kg K), $\rho_{\text{ice}} \approx 927$ kg/m^3, $k_{\text{ice}} \approx 3.2$ W/(m K)
See Winter and Saari (1969) for heat capacity of silicates as a function of temperature.
See Handbook of Chemistry and Physics (Lide, 2003) for temperature dependences for ice.

In the program, k and ρc are defined on half-points, while ρ_f and T are defined on grid points.

Used in Schorghofer and Aharonson (2005) and as part of many other modeling papers.

Bibliography

D. R. Lide, editor. *CRC Handbook of Chemistry and Physics*. CRC Press, 84th edition, 2003.

N. Schorghofer and O. Aharonson. Stability and exchange of subsurface ice on Mars. *J. Geophys. Res.*, 110(E5):E05003, 2005.

M. Siegler, O. Aharonson, E. Carey, M. Choukroun, T.L. Hudson, N. Schorghofer, and S. Xu. Measurements of thermal properties of icy Mars regolith analogs. *J. Geophys. Res.*, 117:E03001, 2012.

D. F. Winter and J. M. Saari. A particulate thermophysical model of the lunar soil. *Astrophys. J.*, 156:1135–1151, 1969.

Part 2

Diffusion of Water Vapor with Phase Transitions

History: developed 2003–2004

1-dimensional diffusion of water vapor; variable diffusivity; irregular grid
3 phases: vapor, free (macroscopic) H_2O ice, H_2O adsorbate
implemented in `vapordiffusioni.f`

2.1 Governing Equations

indices: v ... gas (vapor), f ... free ice (solid), a ... adsorbed water
$\bar{\rho}$ ... mass per total volume, $\bar{J}$ ... vapor flux per total area

conservation of mass:

$$\frac{\partial}{\partial t}(\bar{\rho}_v + \bar{\rho}_f + \bar{\rho}_a) + \nabla \cdot \bar{J} = 0 \tag{2.1}$$

vapor transport: (Landau and Lifshitz, 1987, Vol. VI, §57, §58)

$$J = -D\rho_0 \nabla c \tag{2.2}$$

c ... concentration $c = \rho_v/\rho_0$
ρ_{air} ... total density of air, including humidity
ρ_v ... density of vapor

$$p_v = nkT = \rho_v \frac{k}{m_v} T \tag{2.3}$$

m ... mass of molecule; k ... Boltzmann constant

adsorption: $\bar{\rho}_a = A(p, T)$
The amount adsorbed also changes when ice is present.

ϵ ... porosity (= void space / total volume)
$\epsilon(1 - \rho_f/\rho_{\text{ice}})$ ... fraction of space available to gas
$\bar{\rho}_v = \rho_v \epsilon(1 - \rho_f/\rho_{\text{ice}})$ $\quad$ ρ_v ... vapor density in void space
$\bar{\rho}_f = \rho_f \epsilon$ $\quad$ ρ_f ... ice density in volume not occupied by regolith
$\bar{J} = J\epsilon(1 - \rho_f/\rho_{\text{ice}})$ $\quad$ J ... vapor flux through void area

$\rho_{\text{ice}} \approx 926$ kg/m^3 ... density of ice when it's really cold

Conservation of mass becomes

$$\frac{\partial}{\partial t}\left(\rho_v\left(1-\frac{\rho_f}{\rho_{\text{ice}}}\right)+\rho_f+\frac{1}{\epsilon}\bar{\rho}_a\right)+\partial_z\left(1-\frac{\rho_f}{\rho_{\text{ice}}}\right)J=0$$

$$\frac{\partial}{\partial t}\left[\rho_v\left(1-\frac{\rho_f}{\rho_{\text{ice}}}\right)+\rho_f+\frac{1}{\epsilon}\bar{\rho}_a\right]=\partial_z\left[\left(1-\frac{\rho_f}{\rho_{\text{ice}}}\right)D\partial_z\rho_v\right]$$

introduce $\varphi = 1-\dfrac{\rho_f}{\rho_{\text{ice}}}$ and $\gamma = \dfrac{k}{m}\dfrac{1}{\epsilon}$

$$\partial_t\left(\frac{p}{T}\varphi+\frac{k}{m_v}\rho_f\right)+\gamma\left(\frac{\partial\bar{\rho}_a}{\partial p}\partial_t p+\frac{\partial\bar{\rho}_a}{\partial T}\partial_t T\right)=\partial_z\left[D\varphi\left(\partial_z\frac{p}{T}\right)\right] \tag{2.4}$$

This is an equation for p and ρ_f.

If there is no ice, then

$$\left(\frac{1}{T}+\gamma\frac{\partial\bar{\rho}_a}{\partial p}\right)\partial_t p+\left(-\frac{p}{T^2}+\gamma\frac{\partial\bar{\rho}_a}{\partial T}\right)\partial_t T=\partial_z\left(D\partial_z\frac{p}{T}\right)$$

2.2 Discretizations

2.2.1 Possible discretizations of spatial derivatives:

Note: These spatial discretizations are not necessarily the best possible.

$$\partial_z(a\partial_z b)|_j=\frac{1}{\Delta z^2}\left(a_{j+1/2}(b_{j+1}-b_j)-a_{j-1/2}(b_j-b_{j-1})\right)+O(\Delta z^2) \tag{2.5}$$

or

$$\partial_z(a\partial_z b)|_j=\frac{1}{2\Delta z^2}\left((a_{j+1}+a_j)(b_{j+1}-b_j)-(a_j+a_{j-1})(b_j-b_{j-1})\right)+O(\Delta z^2) \tag{2.6}$$

or

$$\begin{aligned}\partial_z(a\partial_z b)|_j &= a\partial_{zz}b+(\partial_z a)\partial_z b\\ &= \frac{1}{\Delta z^2}\left(a_j(b_{j+1}-2b_j+b_{j-1})+\frac{1}{4}(a_{j+1}-a_{j-1})(b_{j+1}-b_{j-1})\right)+O(\Delta z^2)\end{aligned} \tag{2.7}$$

The most general discretization which is accurate to $O(\Delta z^2)$, rather than just $O(\Delta z)$, is of the following form (mathematica notebook discretization2.nb)

$$\begin{aligned}\partial_z(a\partial_z b)|_j &= \frac{1}{\Delta z^2}(ca_jb_j+(-1-\frac{c}{2})a_{j-1}b_j+(-1-\frac{c}{2})a_{j+1}b_j\\ &\quad -\frac{c}{2}a_jb_{j-1}+\frac{3+c}{4}a_{j-1}b_{j-1}+\frac{1+c}{4}a_{j+1}b_{j-1}\\ &\quad -\frac{c}{2}a_jb_{j+1}+\frac{1+c}{4}a_{j-1}b_{j+1}+\frac{3+c}{4}a_{j+1}b_{j+1})+O(\Delta z^2)\end{aligned} \tag{2.8}$$

Choices (2.6) and (2.7) above correspond to $c = -1$ and $c = -2$, respectively.

Another set of schemes are the ones that do not involve the corner points $a_{j+1}b_{j-1}$ and $a_{j-1}b_{j+1}$. They are of the following form (mathematica notebook discretization3.nb)

$$\begin{aligned}\partial_z(a\partial_z b)|_j &= \frac{1}{\Delta z^2}(-a_j b_j - c a_{j-1} b_j + (-1+c) a_{j+1} b_j + \\ &\quad (1-c) a_j b_{j-1} + c a_{j-1} b_{j-1} + c a_j b_{j+1} + (1-c) a_{j+1} b_{j+1}) + \\ &\quad \left(c - \frac{1}{2}\right) O(\Delta z) + O(\Delta z^2) \qquad (2.9) \\ &= \frac{1}{\Delta z^2}\left[(1-c) a_{j+1}(b_{j+1} - b_j) + c a_{j-1}(b_{j-1} - b_j) + a_j(c b_{j+1} - b_j + (1-c) b_{j-1})\right] + O(\Delta z)\end{aligned}$$

For $c = 1/2$ this reduces to scheme (2.6) above
If starting with complete pore filling, $c > 0$ is required for downward motion of ice table.

On irregular grid: General scheme without corner points (mathematica notebook discretization6.nb)

$$\begin{aligned}\partial_z(a\partial_z b)|_j &= -\frac{2c + (1-2c) h_+/h_-}{h_- h_+} a_j b_j + \frac{-1 + (1-2c) h_+/h_-}{h_-(h_- + h_+)} a_{j-1} b_j + \frac{2c-2}{h_+(h_- + h_+)} a_{j+1} b_j + \\ &\quad + \frac{1 + (1-2c) h_+/h_-}{h_-(h_- + h_+)} a_j b_{j-1} + \frac{1 + (2c-1) h_+/h_-}{h_-(h_- + h_+)} a_{j-1} b_{j-1} + \frac{2c}{h_+(h_- + h_+)} a_j b_{j+1} \\ &\quad + \frac{2 - 2c}{h_+(h_- + h_+)} a_{j+1} b_{j+1} + O(h_+ + h_-) \qquad (2.10)\end{aligned}$$

where $h_+ = z_{j+1} - z_j$ and $h_- = z_j - z_{j-1}$. For $h_+ = h_- = h$ this reduces to (2.9)

2.2.2 Discretization of time derivative:

use eq. (2.4), $A \equiv f$

$$\begin{aligned}\frac{p_j^{n+1}}{T_j^{n+1}} \varphi_j^{n+1} - \frac{p_j^n}{T_j^n} \varphi_j^n + \frac{k}{\mu}\left(\rho_f{}_j^{n+1} - \rho_f{}_j^n\right) + \gamma \left.\frac{\partial f}{\partial p}\right|_j^n (p_j^{n+1} - p_j^n) + \\ + \gamma \left.\frac{\partial f}{\partial T}\right|_j^n (T_j^{n+1} - T_j^n) = \Delta t \left(\partial_z D \varphi \partial_z \frac{p}{T}\right)_j^n \qquad (2.11)\end{aligned}$$

derivatives of the isotherm are not expanded to keep it linear

2.2.3 Complete scheme:

using (2.11) and (2.10)

$$\begin{aligned}\xi_j^{n+1} &= \frac{p_j^n}{T_j^n} \varphi_j^n + \frac{k}{\mu} \rho_f{}_j^n + \gamma \left.\frac{\partial f}{\partial p}\right|_j^n p_j^n - \gamma \left.\frac{\partial f}{\partial T}\right|_j^n (T_j^{n+1} - T_j^n) + \\ &\quad \frac{\Delta t}{\Delta z^2}\left[D_j \varphi_j^n \left(\frac{p_{j+1}^n}{T_{j+1}^n} - 2\frac{p_j^n}{T_j^n} + \frac{p_{j-1}^n}{T_{j-1}^n}\right) + \frac{1}{4}(D_{j+1}\varphi_{j+1}^n - D_{j-1}\varphi_{j-1}^n)\left(\frac{p_{j+1}^n}{T_{j+1}^n} - \frac{p_{j-1}^n}{T_{j-1}^n}\right)\right]\end{aligned}$$

where $\xi^{n+1} = \dfrac{p^{n+1}}{T^{n+1}}\left(1 - \dfrac{\rho_f^{n+1}}{\rho_{\text{ice}}}\right) + \dfrac{k}{\mu}{\rho_f}^{n+1} + \gamma \left.\dfrac{\partial f}{\partial p}\right|^n p^{n+1}$

$p \le p_{sv}(T)$ and $0 \le \rho_f \le \rho_{\text{ice}}$

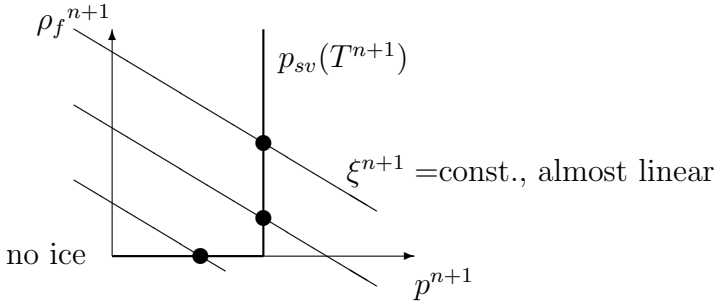

p_{sv} ... saturation vapor pressure

Try $\rho_f^{n+1} = 0 \quad \Rightarrow \quad p^{n+1} = \dfrac{T^{n+1} \cdot \xi^{n+1}}{1 + T^{n+1}\gamma \left.\frac{\partial f}{\partial p}\right|^n}$ and $\rho_f^{n+1} = 0$

If $p^{n+1} > p_{sv}(T^{n+1})$ then $p^{n+1} = p_{sv}(T^{n+1})$ and

$$\rho_f^{n+1} = \frac{\xi^{n+1} - \frac{p_{sv}(T^{n+1})}{T^{n+1}} - \gamma \left.\frac{\partial f}{\partial p}\right|^n p_{sv}(T^{n+1})}{\frac{k}{\mu} - \frac{p_{sv}(T^{n+1})}{T^{n+1}\rho_{\text{ice}}}}$$

introduce $p_{\text{frost}}^{n+1} = p_{sv}(T^{n+1})$

2.2.4 Upper boundary condition:

1) $p(z = 0, t) = p_{\text{atm.}}(t)$
2) $D(z = 0) = D_0$
3) $\varphi_0 = 1$

$$\partial_z \left(D\varphi\partial_z \frac{p}{T}\right)\Big|_{j=0} = \frac{1}{\Delta z^2}\left[D_1\varphi_1\left(\frac{p_2}{T_2} - 2\frac{p_1}{T_1} + \frac{p_{\text{atm}}}{T_{\text{surf}}}\right) + \frac{1}{4}(D_2\varphi_2 - D_0\varphi_0)\left(\frac{p_2}{T_2} - \frac{p_{\text{atm}}}{T_{\text{surf}}}\right)\right] \tag{2.12}$$

for half-shifted grid ($z_2 = 3z_1$):

$$a\partial_{zz}b + (\partial_z a)\partial_z b = \frac{1}{\Delta z^2}\left[a_1\left(\frac{8}{3}b_s - 4b_1 + \frac{4}{3}b_2\right) + \left(-\frac{4}{3}a_s + a_1 + \frac{1}{3}a_2\right)\left(-\frac{4}{3}b_s + b_1 + \frac{1}{3}b_2\right)\right] \tag{2.13}$$

2.2.5 Lower boundary condition:

no vapor flux (impermeable) $J = 0 \quad \Rightarrow \quad \partial_z \rho_v = 0 \quad \Rightarrow \quad \partial_z \dfrac{p}{T} = 0 \quad \Rightarrow \quad \dfrac{p_{N+1}}{T_{N+1}} = \dfrac{p_{N-1}}{T_{N-1}}$

$$\partial_z \left(D\varphi\partial_z \frac{p}{T}\right)\Big|_{j=N} = \frac{1}{\Delta z^2} 2D_N\varphi_N\left(\frac{p_{N-1}}{T_{N-1}} - \frac{p_N}{T_N}\right) \tag{2.14}$$

2.3 Numerical Stability

von Neumann stability analysis has been carried out for various variants of the scheme; this is only relevant for discussion purposes. Typeset notes are available upon request.

Used in Schorghofer and Aharonson (2005)

Bibliography

L. D. Landau and E. M. Lifshitz. *Fluid Mechanics*. Pergamon Press, Oxford, 1987.

N. Schorghofer and O. Aharonson. Stability and exchange of subsurface ice on Mars. *J. Geophys. Res.*, 110(E5):E05003, 2005.

Part 3

Thermal Model for Planar Slopes

Thermal Balance for Planar Slopes; coupled 1D Models plus 0D Atmosphere
For Mars, but easily simplified to airless bodies

Authors & History: Implemented around 2005 by Norbert Schörghofer, with a contribution by Misha Kreslavsky

α ... slope angle

The heat balance on the surface is

$$Q(\alpha) + k \left.\frac{\partial T}{\partial z}\right|_{z=0} = \epsilon\sigma T^4 + (\text{latent heat of CO2 frost}) \tag{3.1}$$

with

$$Q = Q_{\text{solar}}(\alpha) + Q_{\text{IR}}(\alpha) + Q_{\text{scat}}(\alpha) + Q_{\text{land}}(\alpha). \tag{3.2}$$

Q is the incoming radiation from the sun, atmosphere, and visible surfaces, T temperature, z the vertical coordinate, k the thermal conductivity, ϵ emissivity, and σ the Stefan-Boltzmann constant.

The elevation β of the sun above an horizontal horizon is given in terms of geographic latitude λ, declination δ of the sun, and the hour angle h:

$$\sin\beta = \cos\lambda\cos\delta\cos h + \sin\lambda\sin\delta. \tag{3.3}$$

The angle θ of the sun above a sloped surface is

$$\sin\theta = \cos\alpha\sin\beta - \sin\alpha\cos\beta\cos(\Delta a), \tag{3.4}$$

where Δa is the difference between the azimuth of the sun and the azimuth of the topographic gradient. The sun is assumed to be below the horizon if either $\sin\beta < 0$ (horizontal horizon at infinity) or $\sin\theta < 0$ (self shadowing of slope).

The direct solar insolation is

$$Q_{\text{solar}} = \frac{S_0}{R^2}(1-A)(1-f)^{1/\max(\sin\beta, 0.04)}\sin\theta, \tag{3.5}$$

where S_0 is the solar constant, R the distance from the sun in AU, A the albedo, and f due to the extinction in the atmosphere. The nadir optical depth of the atmosphere is $-\ln(1-f)$. The length of the path through the atmosphere is proportional to $1/\sin\beta$ and the transmission is taken to be exponential in this path length. The maximum atmospheric path length $\ell_{\max}$ is limited due

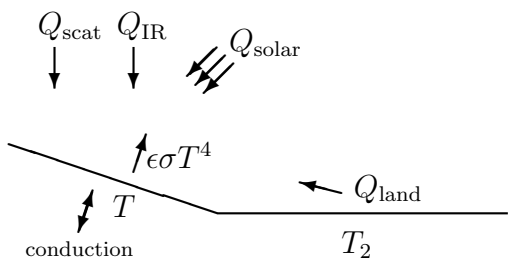

Figure 3.1: Contributions to the heat balance on a slope with surface temperature T.

to the curvature of the planet, $H/\ell_{\rm max} \approx \sqrt{H/2R} \approx 0.04$ for Mars, where H is the scale height of the atmosphere and R the radius of the planet.

Atmospheric emission is approximated by a fraction $f_{\rm IR}$ (typically 2–4%) of noontime insolation and is kept constant throughout a solar day (Kieffer et al., 1977):

$$Q_{\rm IR} = f_{\rm IR} \frac{S_0}{R^2} \cos^2\left(\frac{\alpha}{2}\right) \sin\beta_{\rm noon} \qquad \text{(all day)} \tag{3.6}$$

The slope factor $\cos^2(\alpha/2)$ for the IR emission takes into account that a tilted surface facing a horizontal horizon sees only a restricted portion of the sky. (This approximation fails in the polar regions; in this case, Kieffer et al. (1977) replaces the noontime insolation with the surface frost emission.)

In addition, there is scattered light when $\sin\beta > 0$, which is approximated by

$$Q_{\rm scat} = \frac{1}{2} f_{\rm scat} \frac{S_0}{R^2} \cos^2\left(\frac{\alpha}{2}\right). \tag{3.7}$$

Half of the scattered light is assumed to be lost to space.

The surface reemits radiation in all directions, but receives additional heat from surfaces in its field of view. This emission is weighted according to the incidence angles i and integrated over the spherical angle Ω subtended by the visible land surfaces. If we imagine a horizontal surface at uniform temperature T_2 (Kreslavsky and Head, 2005):

$$Q_{\rm land} = \epsilon_2 \sigma T_2^4 \int \cos i d\Omega = \sin^2\left(\frac{\alpha}{2}\right) \epsilon_2 \sigma T_2^4. \tag{3.8}$$

If one assumes $T_2 = T$ and $\epsilon_2 = \epsilon$, then this term can be brought to the right-hand side of eq. (3.1), leading to an effective emissivity of $\epsilon \cos^2(\alpha/2)$. Otherwise, two 1D models are run simultaneously.

The equation of heat conduction is solved in the subsurface with a semi-implicit Crank-Nicholson scheme on a grid with spatially varying spacings, as described in Part 1 of the User Guide.

Used in Aharonson and Schorghofer (2006); Schorghofer and Edgett (2006)

Bibliography

O. Aharonson and N. Schorghofer. Subsurface ice on Mars with rough topography. *J. Geophys. Res.*, 111(E11):E11007, 2006.

H. H. Kieffer, T. Z. Martin, A. R. Peterfreund, B. M. Jakosky, E. D. Miner, and F. D. Palluconi. Thermal and albedo mapping of Mars during the Viking primary mission. *J. Geophys. Res.*, 82: 4249, 1977.

M. A. Kreslavsky and J. W. Head. Mars at very low obliquity: atmospheric collapse and the fate of volatiles. *Geophys. Res. Lett.*, 32(12):L12202, 2005.

N. Schorghofer and K. S. Edgett. Seasonal surface frost at low latitudes on Mars. *Icarus*, 180(2): 321–334, 2006.

Part 4

Asynchronous Models of Temperature and Long-Term Ice Evolution

Long-term evolution of sub-surface ice using diurnally-resolved temperatures. For Mars, subsurface-atmosphere interactions.

History: Developed 2006–2011 for Mars (where re-charge occurs) and 2013–2015 for asteroids (where impact-gardening occurs)

4.1 Asynchronous Model for Temperature, Impact Stirring, and Ice Loss on Asteroids

Schorghofer (2016) describes this model and applies it to (1) Ceres and (7968) Elst-Pizarro.

4.2 Asynchronous Model for Ice on Mars

Schorghofer (2010) provides a description of this model, which is not repeated here. It couples a diurnally-resolved thermal model with a long-term ice evolution model. Details of the long-term ice evolution model are also described there, which involves a one-sided derivative at the moving ice table. It allows for up to three layers: dry, soil with interstitial ice (plus air), and massive ice with dust. In the current implementation, one of the two interfaces is tracked explicitly.

The model is extensively used in Schorghofer (2007); Schorghofer and Forget (2012) for studies of the Martian Ice Age Cycle.

Bibliography

N. Schorghofer. Dynamics of ice ages on Mars. *Nature*, 449(7159):192–194, 2007.

N. Schorghofer. Fast numerical method for growth and retreat of subsurface ice on Mars. *Icarus*, 208(2):598–607, 2010.

N. Schorghofer. Predictions of depth-to-ice on asteroids based on an asynchronous model of temperature, impact stirring, and ice loss. *Icarus*, 276:88–95, 2016.

N. Schorghofer and F. Forget. History and anatomy of subsurface ice on Mars. *Icarus*, 220(2): 1112–1120, 2012.

Part 5

Surface-bounded Exosphere

Monte Carlo Model of Ballistically Hopping Molecules

History: developed 2012–2015
Core routines are implemented in `montecarlo.f90`

5.1 Introduction

The ballistic trajectories of the molecules in a surface-bounded exosphere is simulated with a Monte-Carlo method. Individual water molecules are launched with Gaussian distributed cartesian velocity components that amount to a random initial azimuth and thermal speed appropriate for the local surface temperature. The model then computes the molecule's impact location and time analytically. An event-driven algorithm is used, where landing and launching events are processed in time-order. Events are scheduled and processed until the molecule is destroyed or lost or until its landing or launch time is beyond the next thermal model time step, when surface temperatures are updated.

Each molecule has a longitude $\mathtt{p}_r[1]$, latitude $\mathtt{p}_r[2]$, status $\mathtt{p}_s$ (on surface =0, in-flight =1, lost or cold-trapped < 0), and time to the next event $\mathtt{p}_t$ (until it arrives on surface or until it will leave the surface). Negative status values can be used to distinguish where it is trapped or how it was lost.

Surface temperatures are calculated with a 1D thermal model.

	M	τ_{dissoc}	
H_2O	18.015	20×3600	Potter and del Duca (1964)
H_2O		1/12.6e-6	Crovisier (1989), normal sun
H_2O		1/23.0e-6	Crovisier (1989), active sun
HDO	19.021		
OH	17.007		
He-4	4.0026	1.9e7	Killen and Ip (1999)
Ar-40	39.962	3.2e6	Killen and Ip (1999)

Table 5.1: Some parameters. τ_{dissoc} = photodissociation time scale at 1 AU

5.2 Ballistic flight on sphere

d ... flight distance
t ... time of flight
$\tau_{\rm res}$ ... surface residence time
$\tau_{\rm dissoc}$ ... photo-destruction time
$v_{\rm esc}$ ... escape speed
v_1 ... velocity along longitude direction
v_2 ... velocity along meridian
v_3 ... vertical velocity component
az ... azimuth
$\Delta\phi$ ... difference in longitude
λ ... latitude
M ... molar mass
$R_{\rm moon}$ ... radius of body

The molecule moves on a plane that goes through the center of sphere/body; the ground track is thus part of a great circle.

Each of the three velocity components is picked from a Gaussian distribution, which involves a scaling factor of $\sqrt{T_{\rm surf}8314.5/M}$. This will lead to a Maxwellian velocity distribution and uniformly distributed launch azimuths. Other probability distributions can be implemented, if desired.

For constant g,

$$t = 2v_3/g \tag{5.1}$$

$$d = \frac{2}{g}v_3\sqrt{v_1^2+v_2^2} \tag{5.2}$$

If $|v| > 0.4v_{\rm esc}$, then use non-uniform gravity formula
If $|v| > v_{\rm esc}$, then gravitational escape

$$az = \texttt{atan2}(v_2, v_1) \tag{5.3}$$

$$\cos(az) = v_2/\sqrt{v_1^2+v_2^2} \tag{5.4}$$

$$\sin\varphi_2 = \sin(d/R_{\rm moon})\cos(\lambda)\cos(az) + \sin(\lambda)\cos(d/R_{\rm moon}) \tag{5.5}$$

$$p_r(2) = \arcsin(\sin\varphi_2) \tag{5.6}$$

$$\cos\varphi_2 = \sqrt{1-\sin^2\varphi_2} \tag{5.7}$$

$$\cos(\Delta\phi) = \frac{\cos(d/R_{\rm moon})\cos(\lambda) - \sin(\lambda)\sin(d/R_{\rm moon})\cos(az)}{\cos\varphi_2} \tag{5.8}$$

Roundoff issues: if $\cos(\Delta\phi) > +1$ then $\cos(\Delta\phi) = +1$; if $\cos(\Delta\phi) < -1$ then $\cos(\Delta\phi) = -1$.

$\Delta\phi = \arccos(\cos(\Delta\phi))$
if $v_1 < 0$, then $\Delta\phi = -\Delta\phi$
$p_r(1) = p_r(1) + \Delta\phi$
if $(\cos\varphi_2 == 0)$ then on pole
$p_r(1)$ is normalized to 0...360°.

$p_t = p_t + t$

5.3 Photo-destruction

Molecules are lost in-flight by photo-destruction (Table 5.1), at a rate of $t/(\tau_{\rm dissoc} R^2)$, where R is the distance from the sun, often approximated by the semi-major axis. Require incident flux $Q > 0$, since this only occurs on the dayside.

5.4 Coriolis effect

The Coriolis effect is incorporated by adding tangential velocities but subtracting the distance the surface has traveled during time of flight.

At launch:

$$v_1 = v_1 - \frac{2\pi R_{\rm moon}}{\rm siderealDay} \cos(p_r(2)) \tag{5.9}$$

After landing:

$$p_r(1) = p_r(1) + t/{\rm siderealDay} \tag{5.10}$$

The Coriolis effect is negligible on the Moon and on Mercury, but noticable on Ceres.

5.5 Event driver

Process events over the time step of the thermal model Δt_T, e.g., one hour

```
if (p_t > dtsec) exit
case(p_s < 0) exit !  not alive
case(p_s==0) !  leaving
   hop once, update p_t
case(p_s==1) !  landing
   if (incoldtrap) then
      p_t = ∞
      cycle
   endif
   evaluate τ_res(T_surf)
   p_t = p_t + τ_res
```

After all events within Δt_T are processed, subtract Δt_T from all times: if ($\mathtt{p_s} >= 0$) $p_t = p_t - \Delta t_T$. (Moving time zero helps avoid truncation errors after a long run.)

5.6 Residence times

E ... sublimation rate/flux
θ ... number of H_2O molecules per area
$\theta_m = 1e19 m^{-2}$ ... areal density of H_2O monolayer
T ... local surface temperature

Temperature also sets the residence time of water molecules on the surface, which is negligible on most of the dayside and very long on most of the nightside. Many models use a binary choice,

where molecules either immediately hop on the day side or reside indefintely on the surface on the night side. This model uses a molecular residence time that depends continuously on temperature instead of a threshold.

For crystalline ice, the average molecular surface residence time only depends on T, but for adsorbed water it is also a function of the adsorbate density θ. The model uses the parametrization $\tau_{\rm res} = c\theta_m/E(T)$, where E is the sublimation rate of pure ice. For pure ice $c = 1$. For example, $c = 1/400$ is reasonable for 0.1 monolayers (Schorghofer and Aharonson, 2014). The functional form is almost the same as using a vibration frequency multiplied by a Boltzmann factor.

For non-condensible species, e.g. He, $\tau_{\rm res} = 0$.

5.7 Non-uniform gravity

ballistic travel distance and flighttime for non-uniform gravity; not suitable for small velocities due to roundoff. Equations based on Vogel (1966) and Kegerreis (2015).

e ... eccentricy of ballistic trajectory
α ... zenith angle of launch velocity, $\alpha = \arctan\left(\sqrt{v_1^2 + v_2^2}/v_3\right)$

$$\gamma = \left(|v|/v_{\rm esc}\right)^2 \tag{5.11}$$
$$a = \frac{R_{\rm moon}}{2(1-\gamma)} \tag{5.12}$$
$$e = \sqrt{1 - 4(1-\gamma)\gamma \sin^2\alpha} \tag{5.13}$$
$$d = 2R_{\rm moon} \arccos\left(\frac{1}{e}(1 - 2\gamma \sin\alpha^2)\right) \tag{5.14}$$
$$E_p = \pi - 2\arctan\left(\sqrt{\frac{1-e}{1+e}}/\tan\frac{d}{4R_{\rm moon}}\right) \tag{5.15}$$
$$t = 2\sqrt{\frac{2a^3}{R_{\rm moon} v_{\rm esc}^2}}(E_p + e\sin E_p) \tag{5.16}$$

Round-off issues:
a) If e is very close to 1, then based on Taylor expansion of (5.13) and (5.14)

$$d = R_{\rm moon} 4\gamma \sin\alpha \tag{5.17}$$
$$E_p = \pi - 2\arctan\left(\sqrt{(1-\gamma)/\gamma}\right) \tag{5.18}$$

b) If $1 - 2\gamma\sin^2\alpha > e$ (horizontal launch), do something, otherwise $d =$ `NaN`

Used in Schorghofer (2014) (uniform gravity) and Schorghofer et al. (2016a,b) (non-uniform gravity).

Bibliography

J. Crovisier. The photodissociation of water in cometary atmospheres. *Astr. Astrophys.*, 213: 459–464, 1989.

J. Kegerreis. Bouncing on the moon. Master's thesis, Durham University, 2015.

R. M. Killen and W.-H. Ip. The surface-bounded atmospheres of Mercury and the Moon. *Rev. Geophys.*, 37(3):361–406, 1999.

A. E. Potter and B. del Duca. Lifetime in space of possible parent molecules of cometary radicals. *Icarus*, 3:103, 1964.

N. Schorghofer. Migration calculations for water in the exosphere of the Moon: Dusk-dawn asymmetry, heterogeneous trapping, and D/H fractionation. *Geophys. Res. Lett.*, 41:4888–4893, 2014.

N. Schorghofer and O. Aharonson. The lunar thermal ice pump. *Astrophys. J.*, 788:169, 2014.

N. Schorghofer, P. Lucey, and J.-P. Williams. Theoretical time variability of mobile water on the moon and its geographic pattern. *Icarus*, 2016a. Submitted.

N. Schorghofer, E. Mazarico, T. Platz, F. Preusker, S.E. Schröder, C.A. Raymond, and C.T. Russell. The permanently shadowed regions of dwarf planet Ceres. *Geophys. Res. Lett.*, 43:6783–6789, 2016b.

U. Vogel. Molecular fluxes in the lunar atmosphere. *Planet. Space Sci.*, 14:1233–1252, 1966.

Part 6

Terrestrial Analogs

1-Dimensional Thermal Model with 0-Dimensional Terrestrial Atmosphere

Sun postion as a function of date is based on Blanco-Muriel et al. (2001), translated into Fortran. It provides the zenith angle and azimuth of the sun, and the Earth-sun distance. Implemented in `sunpos.f90`

6.1 Mauna Kea atmosphere

calculate clear-sky direct and indirect short-wave irradiance on Mauna Kea in W/m^2
mostly based on Nunez (1980), corrected for typos. Implemented in `mk_atmosphere.f90`

Z ... solar zenith angle (radians)
I_0 ... clear-sky direct irradiance; D_0 ... clear-sky diffuse irradiance
R ... Eart-sun distance in AU
m, m' ... optical air mass (unitless)
p_0 ... total pressure (Pa)
w ... precipitable water vapour (cm)
Transmission coefficients:
ψ_{wa} ... water vapor absorption; ψ_{ws} ... water vapor scattering
ψ_{rs} ... Rayleight scattering
ψ_{da} ... dust absorption; ψ_{ds} ... dust scattering

Relative air mass:
simplest approximation: $m = 1/\cos Z$
better approximation (Kasten, 1966):

$$m = \frac{1}{\cos Z + 0.15 \times (93.885 - Z)^{-1.253}} \tag{6.1}$$

if $(m < 0)$, then $m = \infty$
$p_0 = 610$ on Mauna Kea summit
$m' = m \times p_0/1013$

Water vapor:
$w = 0.16$ cm for Mauna Kea, according to www.gemini.edu/sciops/telescopes-and-sites/observing-

condition-constraints/mk-water-vapour-statistics

$$\psi_{wa} = 1 - 0.077(wm)^{0.30} \quad \text{McDonald (1960)} \tag{6.2}$$
$$\psi_{ws} = 1 - 0.025wm \tag{6.3}$$

Rayleigh scattering: 8% at sea level according to Fig 3-3 in Bird and Hulstrom (1981)

$$\psi_{rs} = \exp(-0.08m') \tag{6.4}$$

Aerosols: aerosol optical depth on Mauna Kea $= 0.0084 \times (\lambda/1\mu m)^{-1.26}$, Buton et al. (2013)

$$\psi_{ds} = \exp(-m \times 0.0084 \times 0.5^{-1.26}) \tag{6.5}$$
$$\psi_{da} = \psi_{ds} \quad \text{assumes single scattering albedo of 0.5} \tag{6.6}$$

Direct sunlight:

$$I_0 = \psi_{wa}\psi_{da}\psi_{ws}\psi_{rs}\psi_{ds} \times (\text{solar constant})/R^2 \tag{6.7}$$

(without the last factor, this is the transmittance)

Diffusive sunlight:

$$D_0 = I_0 \cos(Z)\psi_{wa}\psi_{da}\frac{1 - \psi_{ws}\psi_{rs}\psi_{ds}}{2} \tag{6.8}$$

With restricted horizon $D_0 = D_0 \times$(sky size); without obstructions (sky size)=1
Roundoff issue: if ($D_0 <= 0$), then $D_0 = 0$ because of -0

Total short-wavelength flux:

$$F = I_0 \cos Z + D_0 \tag{6.9}$$

Roundoff issue: if ($F <= 0$), then $F = 0$ because of -0

Not included are the sensible heat flux and long-wave downward radiation.

6.2 Dry Valleys of Antarctica

used in Schorghofer (2005)

[To Be Written]

Bibliography

R. E. Bird and R. L. Hulstrom. A simplified clear sky model for direct and diffuse insolation on horizontal surfaces, 1981.

M. Blanco-Muriel, D. C. Alarcón-Padilla, T. López-Moratalla, and M. Lara-Coira. Computing the solar vector. *Solar Energy*, 70:431–441, 2001.

C. Buton et al. Atmospheric extinction properties above Mauna Kea from the Nearby SuperNova Factory spectro-photometric data set. *Astr. & Astrophys.*, 549:A8, 2013.

F. Kasten. *Arch. Meteor. Geophys. Bioklimatol.*, B14:206–223, 1966.

J. E. McDonald. Direct absorption of solar radiation by atmospheric water vapor. *J. Meteor.*, 17: 319–328, 1960.

M. Nunez. The calculation of solar and net radiation in mountainous terrain. *J. Biogeogr.*, 7: 173–186, 1980.

N. Schorghofer. A physical mechanism for long-term survival of ground ice in Beacon Valley, Antarctica. *Geophys. Res. Lett.*, 32:L19503, 2005.